Astron. Astrophys. 330, 311–320 (1998)

ASTRONOMY
AND
ASTROPHYSICS

The SO-to-CS abundance ratio in molecular cirrus clouds

Andreas Heithausen[1], **Uwe Corneliussen**[2], **and Volkmar Großmann**[3]

[1] Radioastronomisches Institut der Universität Bonn, Auf dem Hügel 71, D-53121 Bonn, Germany
[2] I. Physikalisches Institut der Universität zu Köln, Zülpicher Straße 77, D-50937 Köln, Germany
[3] Institut für Astronomie und Astrophysik - Astronomie, Universität Tübingen, Waldhäuser Str. 64, D-72076 Tübingen, Germany

Received 15 July 1997 / Accepted 15 September 1997

Abstract. We have extended our study of sulphur monoxide towards other less opaque cirrus cores and have clearly detected 3 out of 6 sources observed, for the Draco cloud, LVC-127+20, and MBM 32. We find for at least one further cloud (MBM 32) that SO is extended. Assuming that the lines are optically thin we derive column densities of about N(SO)= $5\,10^{12}\,\mathrm{cm}^{-2}$. Based on the visual extinction estimates we derive abundances X(SO)=$2\,10^{-9}$, thus again higher than can be predicted by chemical models with standard assumptions on a low initial S abundance in the gas phase. Our new observations therefore confirm our previous conclusion, that in cirrus clouds sulphur must be essentially undepleted to explain the amount of SO detected.

For MCLD 126.6+24.5 we present an analysis of our extensive SO (N_J = $1_0 \rightarrow 0_1$) mapping. The SO emission reveals clumpy structure of that cloud. We decompose the SO cloud into 17 individual clumps. Those clumps follow the same size-line width relation as high latitude molecular clouds (HLCs) on larger scales. Also, the size-density relation for the SO clouds has the same slope as that for other HLCs found from CO observations.

The clouds detected in SO were also observed in the CS (J = $2 \rightarrow 1$) and ($3 \rightarrow 2$) lines. Only MCLD 126.6+24.5 and MBM 32 were detected in CS. For the most intense SO clump in MCLD 126.6+24.5 we present a detailed study of SO and CS. The abundance ratio of CS and SO ranges from unity for MCLD 126.6+24.5 to less than 0.1 for the other clouds, indicating a low depletion of oxygen in that clouds. Our detailed comparison of CS and SO in MCLD 126.6+24.5 both in position and in velocity indicate that the molecules do not necessarily coexist in the cloud; we find that both molecules are not equally distributed, that the profiles of both molecules look different and that there is no correlation between the column densities of the molecules. Our findings let us suggest that these clouds are inhomogeneous clumpy objects, possibly not well described by simple equilibrium models.

Send offprint requests to: A. Heithausen, Internet: Heith@Astro.Uni-Bonn.De

Key words: ISM: abundances – ISM: clouds – ISM: individual objects: MBM 32, MCLD 126.6+24.5 – ISM: molecules – radio lines: ISM

1. Introduction

Molecular clouds are highly fragmented or clumpy objects. This fragmentation plays a key role in our understanding of the process of star formation (e.g. Scalo 1985). So far, mainly CS and $C^{18}O$ have been used to trace the dense cores in molecular clouds. It is however not always clear whether variations in the column densities of these molecules reflect true physical variations or are just a consequence of chemical abundance variations.

There is increasing evidence that chemical effects cannot be ignored when studying molecular cloud structure (cf. Goldsmith et al. 1991). The study of L134N by Swade (1989) revealed that abundance variations exist over short distances in molecular clouds, e.g. "the observations in L134N indicate that SO and CS do not coexist over a significant fraction of the core region" (Swade 1989). The observations of several molecular species in the Orion molecular cloud by Ungerechts et al. (1995) give similar results. Whereas abundance variations in Orion can easily be explained by variations in the interstellar radiation field, this explanation does not hold for molecular clouds far from actively star forming regions (cf. Gerin et al. 1997).

CS and SO are molecules which are well suited to study chemical abundance variations in molecular clouds. First, they react sensitively to elemental varition inside the clouds: oxygen rich clouds have higher SO abundances whereas carbon rich clouds should have higher CS abundances (Millar & Herbst 1990). Second, because their permanent electric dipole moments are similar (μ(SO) = 1.55debye and μ(CS) = 1.958debye, Swade 1989) they trace similar excitation conditions. Third, they have mm-wave transitions separated only by a few GHz, thus these lines can be observed with the same radio telescope with similar angular resolutions, so that different

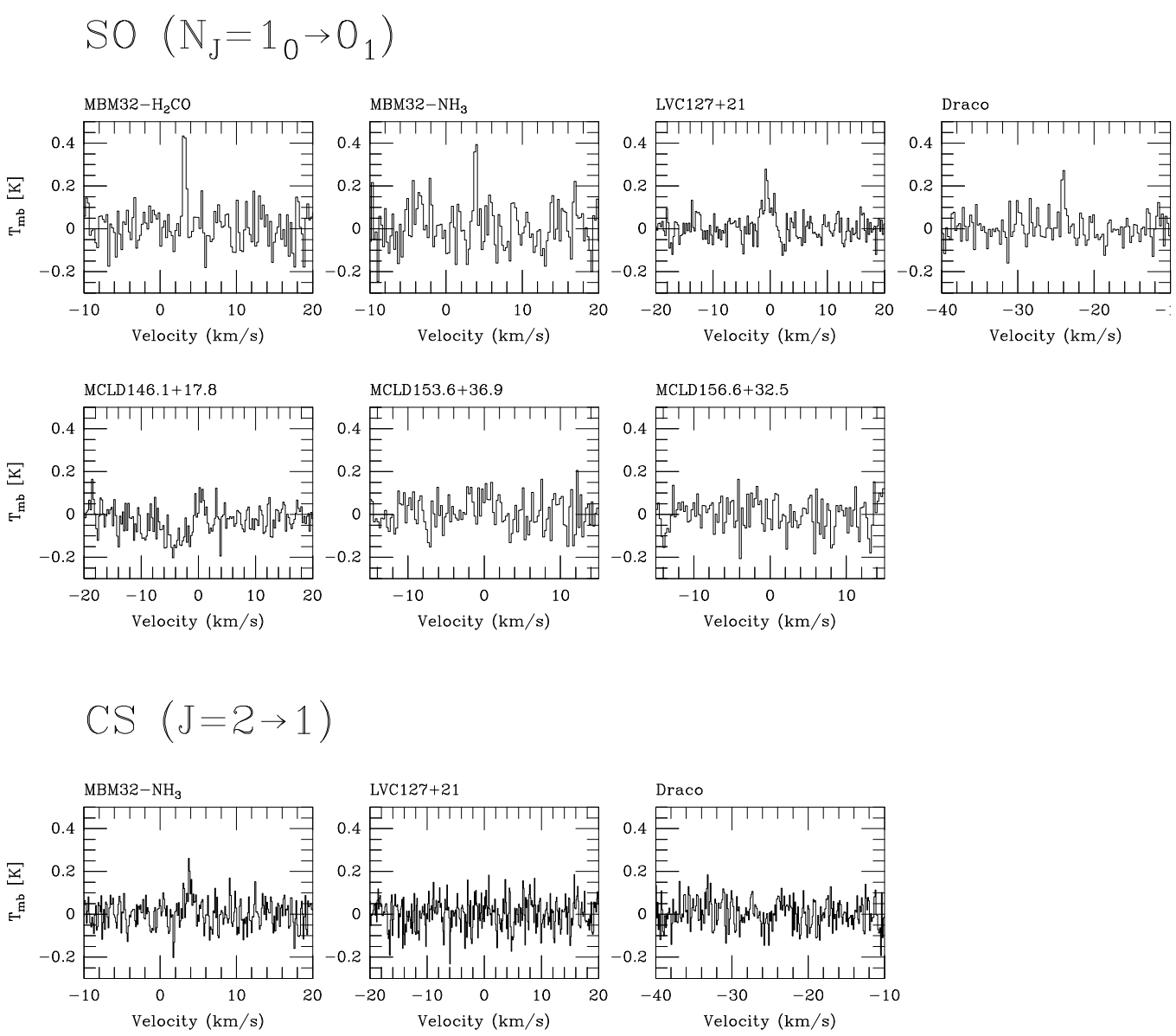

Fig. 1. Spectra of the SO ($N_J = 1_0 \rightarrow 0_1$) transition for the different newly observed clouds (top). Line parameters derived from a gaussian fit to the spectra are listed in Table 2. Clouds detected in SO were also observed in CS; the corresponding CS ($J = 2 \rightarrow 1$) spectra are displayed on the bottom of the figure.

beam coupling does not complicate the interpretation of the observations.

For our study we have selected several high latitude molecular clouds, previously studied in several molecular transitions, as CO (Heithausen et al. 1993), NH_3 and/or H_2CO (Heithausen et al. 1987, Mebold et al. 1987, Boden & Heithausen 1993). This paper is a continuation of our study of SO in galactic cirrus clouds (Heithausen et al. 1995, hereafter Paper I). The purpose of this paper is twofold: first, we present the results of our extended search for the SO ($N_J = 1_0 \rightarrow 0_1$) line towards less opaque cirrus cores, showing that SO might be a good tracer for the denser structures in molecular clouds (Sect. 3). We also analyse the structure of one cloud core seen in SO ($N_J = 1_0 \rightarrow 0_1$). Second, we discuss in detail the distribution and excitation conditions of SO in comparison to CS in one cirrus cloud, MCLD 126.6+24.5 (Sect. 4). These observations reveal that the structure of molecular cirrus clouds is not simple, but rather is very clumpy as already found for dark clouds. In a subsequent paper (Großmann et al. 1997) we will discuss the chemical structure of MCLD 123.5+24.9, where we observed varying chemical abundances over a linear distance of only a few 0.01 pc. There, we will describe the detection of H_2S, H_2CS, N_2H^+, HC_3N, HCS^+, and multi-transition CS and SO observations for that cloud.

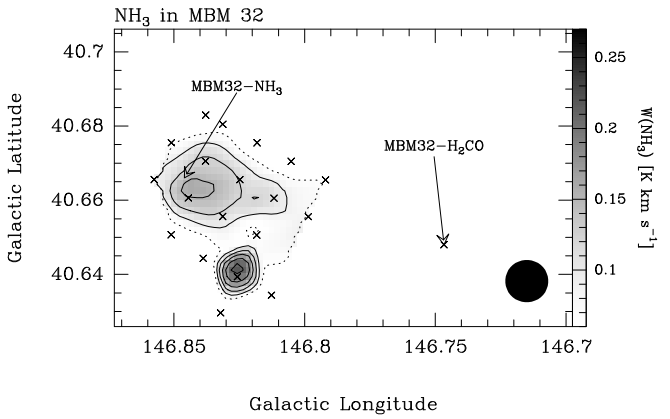

Fig. 2. The dense core in MBM 32 as observed in the NH_3 (1,1) transition with the MPIfR 100 m telescope. The two positions were SO has been detected are marked MBM 32-NH_3 and MBM 32-H_2CO. The one named MBM 32-NH_3 is observed towards the position with the strongest ammonia emisson, the one named MBM 32-H_2CO towards the position with the deepest H_2CO $J_{ka,kc} = 1_{1,0} \rightarrow 1_{1,1}$ absorption (Heithausen et al. 1987).

2. Observations

The observations of the SO ($N_J = 1_0 \rightarrow 0_1$) transition at 30.001539 GHz were conducted in January 1995 with the MPIfR 100 m telescope equipped with a HEMT receiver with a total system temperature of about 130 K (SSB). At this frequency the beam size is 30″. The pointing was checked every 2 hours and was better than 5″. The observing program consisted of a continuation of the mapping of MCLD 126.6+24.5 and a search for SO towards other cirrus clouds. For the mapping the integration time per position was 5 min on source and 5 min on an emission free position resulting in a rms in single spectra better than 0.34 K (T_{mb}). For the search program the integration time was between 1 and 2 hours giving rms of better than 0.1 K. The spectra were obtained with the 1024 channel autocorrelation spectrometer with a velocity resolution of 0.12 km s^{-1} and were calibrated using continuum cross scans on W3(OH) which has a λ 1 cm flux density of 3.6 Jy (Ott et al. 1994). A summary of observational parameters is given in Table 1. The results from a gaussian analysis of the spectra are listed in Table 2.

Additionally, we have observed the CS ($J = 2 \rightarrow 1$) and ($J = 3 \rightarrow 2$) lines in all clouds, where we detected SO, and in MCLD 126.6+24.5 the SO ($N_J = 4_3 \rightarrow 3_2$) and ($N_J = 3_2 \rightarrow 2_1$) transitions using the IRAM 30 m telescope in May 1995 and July 1996. Both transitions of CS and SO were observed simultaneously using SIS receivers with average system temperatures of 250 K at 100 GHz and 360 K at 140 GHz. For MCLD 126.6+24.5 we also obtained $C^{18}O$ ($J = 2 \rightarrow 1$) data with a SIS receiver of $T_{sys} = 650$ K. We used the autocorrelation spectrometer with a velocity resolution of 0.03 km s^{-1} at 100 GHz, 0.02 km s^{-1} at 140 GHz, and 0.14 km s^{-1} at 219 GHz, respectively. Spectra were integrated until the resulting rms was better than 0.1 K (T_{mb}) for all lines. We observed with a sampling of 15″, the beam sizes are 24″ at 100 GHz, 17″ at 140 GHz, and 11″ at 219 GHz. Efficiencies for the IRAM 30 m telescope, taken from Kramer & Wild (1994), are listed in Table 1.

3. Results of the SO observations

For this study we have selected several CO clouds from the CfA high-latitude CO survey (Heithausen et al. 1993) and, additionally, the Draco cloud, because for these sources we have further information on column densities based on other molecular line observations. Fig. 1 shows the results of our search for the SO ($N_J = 1_0 \rightarrow 0_1$) transition towards these cirrus clouds. The line is clearly detected towards 4 positions in three indiviual clouds. Towards MCLD146.1+17.8 the observations have to be extended to confirm this weak feature which is at the proper velocity, 0.43 km s^{-1} as obtained from CO ($J = 3 \rightarrow 2$) observations (Heithausen 1996).

3.1. MBM 32

MBM 32 is one of the first cirrus clouds where H_2CO and NH_3 were detected (Heithausen et al. 1987, Mebold et al. 1987). Formaldehyde was found to be extended over several arcmins. In Fig. 2 we present the results of extensive observations of the (1,1) inversion transition of ammonia (for details on the observations see Schreiber et al. 1993). Besides the clump presented in that figure, ammonia was found towards several other positions; due to the week lines, however, no complete map could be obtained in a reasonable amount of observing time. Based on the ammonia observations Schreiber et al. determined a kinetic temperature of $T_{kin} = 24^{+10}_{-5}$ K.

In our search for SO we obtained 2 spectra towards MBM 32, one towards the position with the strongest NH_3 emission, the other towards the position with the deepest H_2CO absorption. Both spectra show emission lines of about 0.4 K (s. Fig. 1). It is likely that also in this source SO is extended over several arcmins. To derive SO column densities we adopt excitation temperatures of $T_{ex} = 5$ K and assume that the lines are optically thin; adopting $T_{ex} = 10$ K leads to an increase of a factor of 2 in column densities. We derive a total SO column density of N(SO) = 4.5 10^{12} cm^{-2} towards MBM 32-NH_3 and of N(SO) = 5.9 10^{12} cm^{-2} towards MBM 32-H_2CO.

Using star counts Heithausen & Mebold (1989) derived averaged visual extinctions of $A_V = 0.4$ mag for MBM 32 (also catalogued as LBN691) for an area covering about 1 deg^2 and a peak value of $A_V = 0.6$ mag for the inner 0.08 deg^2. Due to the low number of stars at high latitudes this method is however not sensitive to derive proper extinctions for small areas as that covered by the SO beam. Multi-transition CO and NH_3 observations at higher angular resolution confirm, however, that the low extinction is representative for even smaller areas of MBM 32 (Schreiber et al. 1993). Also, our observations indicate that SO is extended towards MBM 32. Therefore, the SO column density as well as the extinction might be representative for larger portions of the cloud. Even if the visual extinction increases towards the SO position to $A_V = 2$ mag, the abundance of SO

Table 1. Observational parameters

Molecule	Transition	Frequency (GHz)	Telescope	beam ($''$)	η_{mb}	Δv ($\mathrm{km\,s^{-1}}$)
(1)	(2)	(3)	(4)	(5)	(6)	(7)
SO	$N_J = 1_0 \rightarrow 0_1$	30.001539	MPIfR 100 m	30	0.42	0.122
SO	$N_J = 3_2 \rightarrow 2_1$	99.299883	IRAM 30 m	24	0.70	0.029
SO	$N_J = 4_3 \rightarrow 3_2$	138.178641	IRAM 30 m	17	0.58	0.021
CS	$J = 2 \rightarrow 1$	97.980968	IRAM 30 m	24	0.70	0.030
CS	$J = 3 \rightarrow 2$	146.969049	IRAM 30 m	17	0.52	0.020
$C^{18}O$	$J = 2 \rightarrow 1$	219.560327	IRAM 30 m	11	0.41	0.137

Remarks: Column 7 gives the velocity resolution of the auto correlation spectrometer.

Table 2. Search positions and SO ($N_J = 1_0 \rightarrow 0_1$) and CS ($J = 2 \rightarrow 1$) line parameters for the newly observed cirrus clouds

			SO ($N_J = 1_0 \rightarrow 0_1$)			CS ($J = 2 \rightarrow 1$)		
Source	l ($^\circ$)	b ($^\circ$)	$T_{mb}(rms)$ (K)	v_{LSR} ($\mathrm{km\,s^{-1}}$)	Δv ($\mathrm{km\,s^{-1}}$)	$T_{mb}(rms)$ (K)	v_{LSR} ($\mathrm{km\,s^{-1}}$)	Δv ($\mathrm{km\,s^{-1}}$)
Draco	89.530	38.400	0.31 (0.057)	−24.05 (0.05)	0.46 (0.11)	(0.07)	–	–
LVC 127+20	128.250	20.750	0.18 (0.05)	−0.52 (0.14)	1.87 (0.30)	(0.07)	–	–
MCLD146.1+17.8	146.070	17.750	0.16[a] (0.07)	–	–			
MBM 32–H_2CO	146.747	40.648	0.51 (0.083)	3.17 (0.04)	0.50 (0.09)			
MBM 32–NH_3	146.846	40.665	0.48 (0.10)	3.88 (0.04)	0.41 (0.16)	0.22 (0.06)	3.84 (0.02)	0.45 (0.1)
MCLD153.6+36.9	154.210	36.375	(0.077)	–	–			
MCLD156.6+32.5	156.643	32.500	(0.074)	–	–			

Remarks: All values have been obtained from a gaussian fit to the spectra which were smoothed by a Hanning filter. Numbers in brackets are formal errors from the gaussian fits. a: this upper limit has been derived by assuming that the weak feature at $v_{LSR} = 0\,\mathrm{km\,s^{-1}}$ is an actual SO line.

is X(SO)=2 10^{-9}, similarly high as for MCLD 126.6+24.5 and MCLD 123.5+24.9 (cf. Paper I).

3.2. LVC 127+20

LVC 127+20 has been studied by Meyerdierks et al. (1990) in CO and H_2CO. A complete CO map is presented by Heithausen et al. (1993, their cloud # 15). Meyerdierks et al. find high abundances for the molecules they observed. They estimate the visual extinction to be 0.75 mag to the peak position where they found formaldehyde. We observed SO towards the position with the strongest formaldehyde absorption. Similarly as for MBM 32 we adopt an excitation temperature for the SO ($N_J = 1_0 \rightarrow 0_1$) line of T_{ex} = 5K and assume that the line is optically thin. We then derive a total SO column density of N(SO)=7.8 10^{12} $\mathrm{cm^{-2}}$. With the visual extinction estimate and a normal gas-to-dust ratio this column density translates to a SO abundance of X(SO)=1 10^{-9}.

3.3. The Draco cloud

The Draco cloud is one of a few molecular clouds in high galactic latitudes with peculiar velocities, -24 $\mathrm{km\,s^{-1}}$, compared to ± 10 $\mathrm{km\,s^{-1}}$ for most of the other. Mebold et al. (1985) speculate that it might be associated with HI high-velocity clouds. They found extensive CO emission and, towards several positions, H_2CO absorption. We observed SO towards the position where Mebold et al. (1987) detected ammonia. Towards this position Mebold et al. (1985) estimate about 2 mag visual extinction. Adopting T_{ex} = 5K and optically thin emission we derive a total SO column density of N(SO)=3.3 10^{12} $\mathrm{cm^{-2}}$. With the visual extinction estimate and a normal gas-to-dust ratio this column density translates to a SO abundance of about X(SO)=2 10^{-9}.

3.4. MCLD 126.6+24.5

In Fig. 3 we show the results of our extensive mapping program towards MCLD 126.6+24.5. Totally 100 spectra in the SO ($N_J = 1_0 \rightarrow 0_1$) line were taken. In contrast to assertions by Turner (1995) that the structure of dense cores in high-latitude molecular clouds is simple and symmetric, our mapping of the core in MCLD 126.6+24.5, which is one of Turner's target sources, shows the complicated structure of that core, which is neither simple nor symmetric. More obviously, the channel maps reveal the clumpy structure of SO in that cloud, which is similarly seen in CO observations on a larger scale (Corneliussen 1996).

To quantify this structure we have decomposed the SO ($N_J = 1_0 \rightarrow 0_1$) data cube using the GAUSSCLUMP algorithm developed by Stutzki & Güsten (1990). Results of that analysis are presented in Table 3. The SO cloud was subdivided

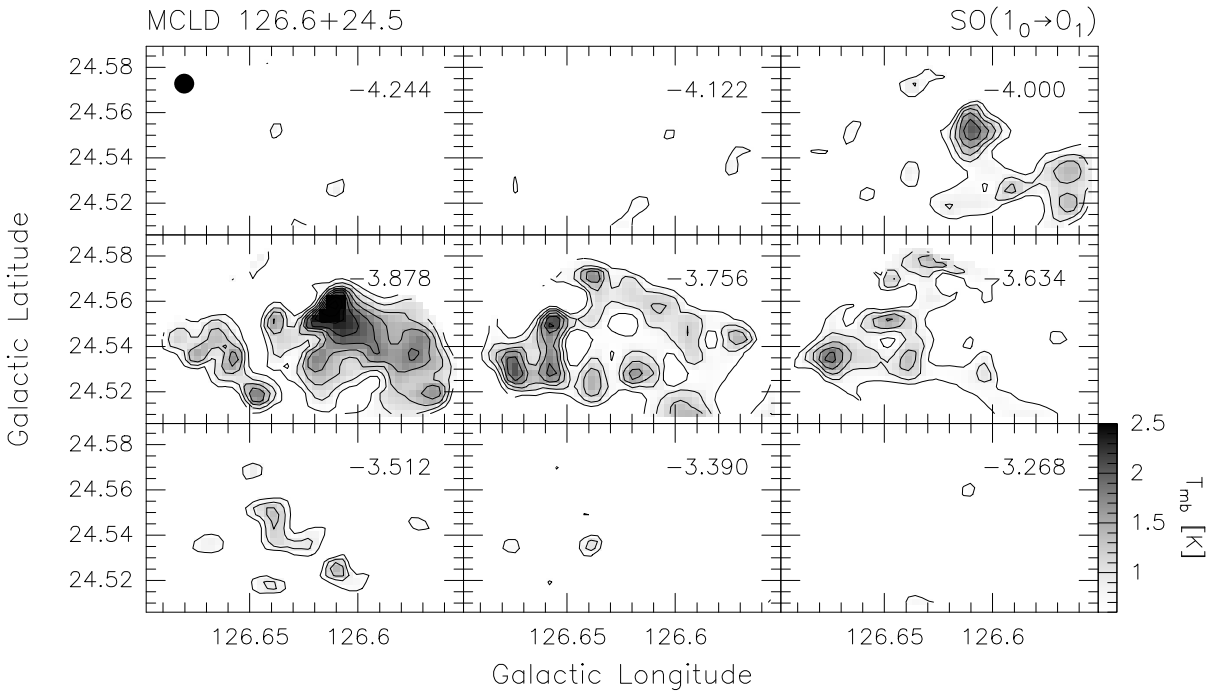

Fig. 3. Channel maps of the SO (N_J = $1_0 \rightarrow 0_1$) line for MCLD 126.6+24.5. Contours are every 0.3 K km s^{-1} (1σ) starting at 0.6 K km s^{-1}. The beam size is indicated at the top left channel map, the centre velocity of each channel at the top right corner of each map. Channels are 0.122 km s^{-1} wide.

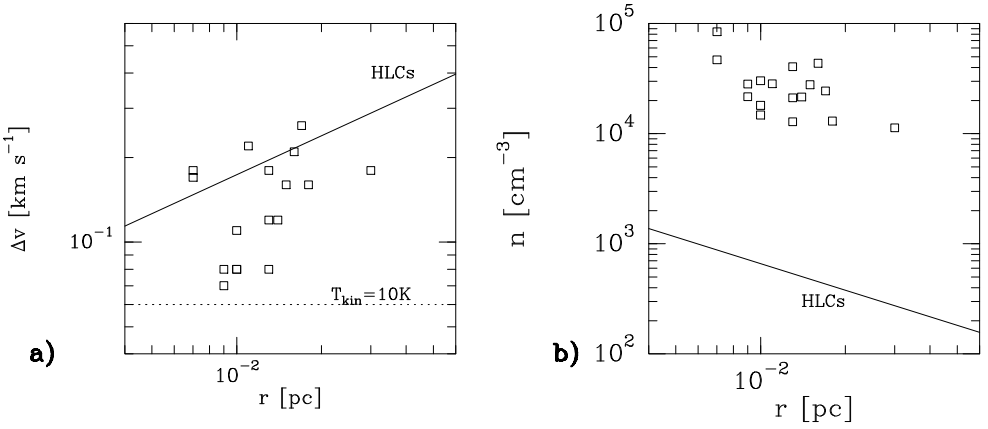

Fig. 4a and b. Size-line width (**a**) and size-density (**b**) relations for the SO clumps in MCLD 126.6+24.5. The solid lines are no fits to the data, but the correlations found for high latitude molecular clouds (Heithausen 1996). The dotted line in (**a**) marks the thermal line width for T_{kin} = 10 K.

into 17 individual clumps. Table 3 lists the number of the clump in column 1, the galactic coordinates in columns 2 and 3, and the centre velocity of the respective clump in column 4. Column 5 gives the velocity full width at half maximum of the clumps deconvolved from the instrumental velocity resolution. We adopt a distance of 100 pc to MCLD 126.6+24.5. The size listed in column 6 is $D = \sqrt{FWHMx * FWHMy}$, deconvolved from the intrinsic beam width of the telescope. To determine the mass we have adopted that the SO (N_J = $1_0 \rightarrow 0_1$) line is optically thin, T_{ex} = 5 K, and an abundance of $X(SO) = 10^{-9}$. The density is the peak volume density of a gaussian density distribution along the line of sight with a full width at half maximum of D.

Fig. 4a and b give the size line-width and the size-density relation for the SO clumps in comparison to the relation for high-latitude molecular clouds as found by Heithausen (1996). The SO clumps fit nicely to that size-line width relation. It is interesting to note that the line-widths of some of the clumps are close to the thermal line width for a SO clump of kinetic temperature 10K.

The size-density relation for the SO clumps (s. Fig. 4b) has a similar slope but a large offset compared to the relation for high-latitude molecular clouds (HLCs) on larger scales (Heithausen 1996). This offset is possibly mostly induced by the different definitions of volume density for the objects. The definition applied here assumes a gaussian density distribution along the line of sight; the volume density is therefore the peak density of the gaussian distribution. The volume density for the HLCs on larger scales is an average density for the cloud assuming that its

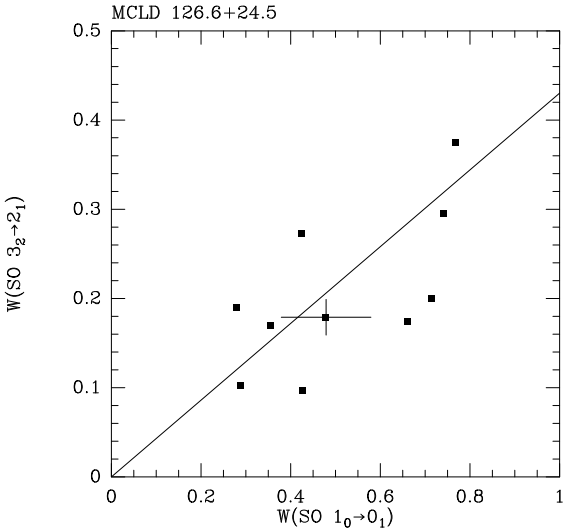

Fig. 5. Comparison of the integrated line temperature of the $N_J = 1_0 \rightarrow 0_1$ and $3_2 \rightarrow 2_1$ transitions of SO in MCLD 126.6+24.5. The cross represents a 1 σ errorbar for the data. The line indicates the ratio of the average SO spectra (see Table 4).

mass is equally distributed over the volume which is determined from the area covered by the clouds up to the detection limit. Both definitions are intrinsically not comparable. Furthermore, the SO lines trace denser gas than the CO ($J = 1 \rightarrow 0$) line does, therefore our SO observations are biased to higher density gas. Nevertheless, the correlation for SO on the one side, and CO on the other follow the same slope, indicating a similar cause for the relation which is possibly related to the fractal structure of interstellar clouds (Elmegreen & Falgarone 1996).

3.5. Excitation of sulphur monoxide in MCLD 126.6+24.5

In Paper I we were only able to derive lower limits for the SO column densities for MCLD 126.6+24.5 and MCLD 123.5+24.9 because there were indications that the $N_J = 1_0 \rightarrow 0_1$ lines were optically thick. In the following we will concentrate on the most intense SO ($N_J = 1_0 \rightarrow 0_1$) clump in MCLD 126.6+24.5 (#1 in Table 3) and discuss the excitation of SO. The centre of the clump is located at $\Delta l = -210''$ and $\Delta b = 60''$ relative to $(l, b) = (126.^\circ675, 24.^\circ535)$. Because we were able to obtain the line strengths of three transitions, we are able to derive better estimates on the excitation condition for SO.

In Table 4 we list representative values for the three observed SO transitions. The first values are for the averaged line profile of the clump centred at ($\Delta l = -210''$,$\Delta b = 60''$); only those positions were averaged where the two CS and the three SO transitions were observed. The second values are for the peak position of that clump. The comparison of the $N_J = 1_0 \rightarrow 0_1$ and $3_2 \rightarrow 2_1$ transitions of SO in MCLD 126.6+24.5 gives $\frac{W(1_0 \rightarrow 0_1)}{W(3_2 \rightarrow 2_1)} = 0.43 \pm 0.06$ for most of the observed positions (see Fig. 5).

Table 3. Parameters of SO ($N_J = 1_0 \rightarrow 0_1$) clumps in MCLD 126.6+24.5

#	l	b	v (km s^{-1})	Δv (km s^{-1})	Size (pc)	Mass ($M_\odot$)	Density (cm^{-3})
(1)	(2)	(3)	(4)	(5)	(6)	(7)	(8)
1	126.6093	24.5529	-3.89	0.21	0.033	0.12	43133
2	126.6583	24.5464	-3.76	0.18	0.026	0.06	40233
3	126.6714	24.5311	-3.71	0.16	0.031	0.06	27549
4	126.5758	24.5361	-3.88	0.18	0.060	0.20	11182
5	126.6368	24.5711	-3.71	0.12	0.027	0.04	21359
6	126.6440	24.5210	-3.84	0.12	0.027	0.03	20982
7	126.6183	24.5288	-3.85	0.26	0.035	0.08	24239
8	126.6378	24.5486	-3.86	0.07	0.018	0.01	27979
9	126.6575	24.5333	-3.87	0.17	0.013	0.02	83306
10	126.6095	24.5238	-3.55	0.11	0.019	0.02	29934
11	126.5953	24.5102	-3.75	0.16	0.036	0.05	12894
12	126.6398	24.5350	-3.61	0.08	0.026	0.02	12705
13	126.6838	24.5436	-3.88	0.22	0.023	0.03	28093
14	126.5917	24.5266	-4.01	0.08	0.020	0.01	17903
15	126.5698	24.5440	-3.74	0.18	0.015	0.01	46342
16	126.6354	24.5726	-4.01	0.08	0.018	0.01	21414
17	126.6457	24.5781	-3.88	0.08	0.021	0.01	14619

Remarks: Size and line width are full width at half maximum of the correponding gaussian fit deconvolved from the intrinsic beam width of the telescope and the intrinsic velocity resolution of the spectrometer, resp.

To determine H_2 volume densities, $n(H_2)$, and SO column densities, N(SO), we used an escape probability model (Walmsley, priv. comm.) to match the observed SO line strength. This model predicts line temperatures for the $3_2 \rightarrow 2_1$ and $4_3 \rightarrow 3_2$ transitions matching those observed for a wide range of volume and column densities. So, based on these two transitions alone no estimate on the SO excitation can be made. The $1_0 \rightarrow 0_1$ transition combined with both higher transitions, however, allows the parameter space to be limited. We find that volume densities of about $1\,10^4$ cm^{-3} are necessary to match the observed line strengths for all three transitions of both the peak and averaged spectra. The column densities are then N(SO)=$1.5\,10^{13}$ cm^{-2} for the whole clump and N(SO)=$3.0\,10^{13}$ cm^{-2} for the peak position, respectively, confirming the values determined in Paper I.

4. Results of the CS observations

For all clouds detected in the SO ($N_J = 1_0 \rightarrow 0_1$) line we were able to obtain complementary CS ($J = 2 \rightarrow 1$) observations. Only MBM 32 and MCLD 126.6+24.5 were detected in CS (s. Fig. 1 and Figs. 6 and 7). Values of the observations are listed in Table 2 and 4. For LVC 127+20, MBM 32 and the Draco cloud we obtain spectra towards single positions, for MCLD 126.6+24.5 we obtained a map of the SO clump discussed in the previous section.

The weak CS ($J = 2 \rightarrow 1$) line detected towards MBM 32 is consistent with the non-detection of that molecule towards 30 positions in that cloud by Reach et al. (1995); the rms of

Table 4. Comparison of CS and SO in MCLD 126.6+24.5

Molecule	Transition	T_{mb} (K)	rms (K)	v_{LSR} (km s^{-1})	Δv (km s^{-1})	N^b (10^{13} cm^{-2})	n^b (cm^{-3})
(1)	(2)	(3)	(4)	(5)	(6)	(7)	(8)
Average values							
SO	$N_J = 1_0 \rightarrow 0_1$	1.72	0.13	−3.88 (0.01)	0.26 (0.02)	$1.5^{+1.5}_{-0.5}$	$(0.3 - 3.0)\,10^4$
SO	$N_J = 3_2 \rightarrow 2_1$	0.71	0.06	−3.84 (0.01)	0.30 (0.01)		
SO	$N_J = 4_3 \rightarrow 3_2$	0.33	0.05	−3.87 (0.01)	0.25 (0.03)		
CS	$J = 2 \rightarrow 1$	0.68	0.03	−3.78 (0.01)	0.41 (0.01)	$2.5^{+5.5(c)}_{-1.7}$	$1.0\,10^{4(c)}$
CS	$J = 3 \rightarrow 2$	0.25	0.03	−3.78 (0.01)	0.37 (0.03)		
Single position[a] at $\Delta l = -210''$, $\Delta b = 60''$							
SO	$N_J = 1_0 \rightarrow 0_1$	2.68	0.24	−3.90 (0.01)	0.26 (0.03)	3^{+2}_{-1}	$(0.3 - 3.0)\,10^4$
SO	$N_J = 3_2 \rightarrow 2_1$	1.25	0.07	−3.88 (0.01)	0.27 (0.01)		
SO	$N_J = 4_3 \rightarrow 3_2$	0.66	0.09	−3.90 (0.01)	0.26 (0.02)		
CS	$J = 2 \rightarrow 1$	0.75	0.08	−3.80 (0.01)	0.40 (0.01)	$2.5^{+5.5(c)}_{-1.7}$	$1.0\,10^{4(c)}$
CS	$J = 3 \rightarrow 2$	0.31	0.09	−3.83 (0.02)	0.35 (0.05)		

Remark: Line parameters are derived from a gaussian analysis of the spectra. Numbers in brackets are formal error from the fits. a) Values are for spectra smoothed to an angular resolution of 30″. b) Volume and column densities are derived from an excitation analysis of the transitions using escape propability models for SO and CS (s. text) adopting T_{kin} = 12 K. c) The CS column density estimate is based on the range for n(H$_2$) taken from SO excitation conditions.

our spectra was slightly better and the angular resolution was higher than for the observations by Reach et al. The comparison of the observations indicate that the CS ($J = 2 \rightarrow 1$) emission has a low beam filling factor which is indicative of clumping in MBM 32.

One could argue that the non-detection of the CS ($J = 2 \rightarrow 1$) line towards LVC 127+20 and the Draco cloud are due to possibility that the line is not excited in those clouds. The excitation conditions for SO and CS are however similar due to the fact that their dipole moments are similar. Furthermore, both clouds are detected in the NH_3 (1,1) inversion line (Mebold et al. 1987, Meyerdierks priv. comm.). The excitation conditions should therefore be sufficient to excite the CS ($J = 2 \rightarrow 1$) line. We therefore conclude that the non-detecion of CS is due to a low CS abundance.

To derive column densities for MBM 32 and upper limits for LVC 127+20 and the Draco cloud we adopt the same excitation temperature as for the SO line, T_{ex} = 5 K, and assume that the line is optically thin. For MBM 32 we derive N(CS)=0.7 10^{12} cm^{-2}, and for LVC 127+20 and the Draco cloud N(CS)$<$ 0.4 10^{12} cm^{-2}, assuming the same line width as for the SO ($N_J = 1_0 \rightarrow 0_1$) transitions and a line temperature of less than $2 \times rms$.

For MCLD 126.6+24.5 the integrated CS (2→1) map does not resemble such a well defined clump as visible in the corresponding SO map. It shows more elongated filament-like structures (Fig. 7). Table 4 lists the CS line parameters derived from gaussian analysis of the peak SO position and an average of the SO whole clump. The corresponding spectra are displayed in Fig. 6. To determine H_2 volume densities, n(H$_2$), and CS column densities, N(CS), we used an escape probability model (Stutzki & Güsten 1990) to match the observed CS line strength. This model predicts line temperatures for the $3 \rightarrow 2$ and $2 \rightarrow 1$ transitions matching those observed for a wide range of volume and column densities. So, based on these two transitions alone no estimate on the CS excitation can be made. To derive the CS column density we therefore adopt that the H_2 density is in the range found for SO n(H$_2$) = $(0.3 - 3.0)\,10^4$ cm^{-3}. For that volume density a CS column density in the range of $(0.8 - 8.0)\,10^{13}$ cm^{-3} is necessary to match the observed line temperatures.

For this excitation analysis only collisions of H_2 and CS have been taken into accound. Drdla et al. (1989) predict that in diffuse clouds CS can significantly be excited by collisions with electrons if the fraction of free electrons is high enough. In their models they show that the ratio of the $J = 2 \rightarrow 1$ to $J = 3 \rightarrow 2$ transition is a good tracer of this effect: A high ratio is an indication of high electron fraction. The ratio we find here is however low, and we therefore conclude that electrons play no major role to excite the CS molecule in MCLD 126.6+24.5.

Based on the CS ($J = 2 \rightarrow 1$) line alone and adopting LTE conditions with T_{ex} = 5 K we yield a total CS column density of N(CS)=2 10^{12} cm^{-2}, which is even lower than the (uncertain) value determined based on the escape probabilty model. Only observations of higher CS transitions can help to overcome the difficulty in the determination of the CS column density.

5. Discussion

Table 5 summarizes the column density estimates for CS and SO in the clouds observed. For LVC 127+20, MBM 32 and the Draco cloud we derive abundance ratio of CS and SO of $\frac{N(\mathrm{CS})}{N(\mathrm{SO})} \leq 0.15$. The abundance ratio for MCLD 126.6+24.5 is uncertain, but possibliy also as low as that for the previously mentioned clouds.

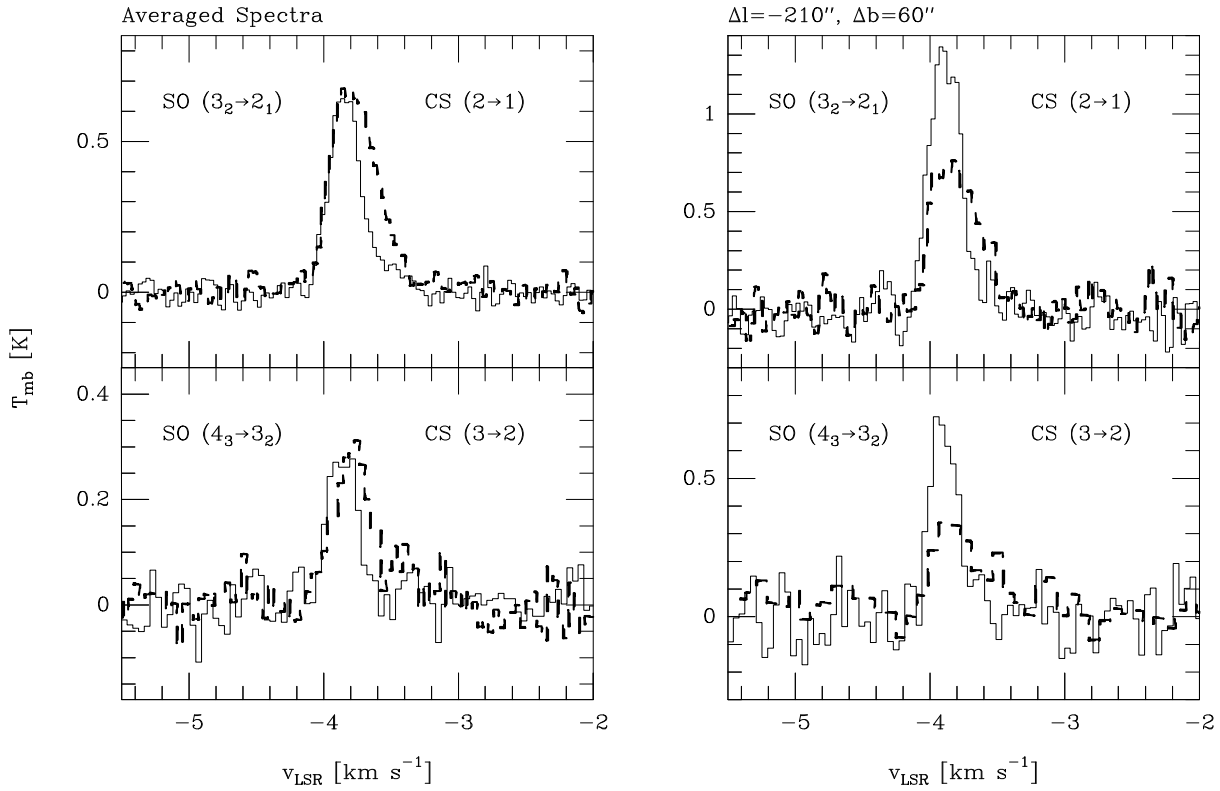

Fig. 6. Comparison of CS and SO spectra in MCLD 126.6+24.5. On the left, spectra averaged over the clump # 1 are displayed, on the right, the spectra at the center position of that clump are shown. Dashed line are CS spectra, solid line SO spectra.

For MCLD 126.6+24.5 we have the possibility to compare the ratio of both molecules over a wider area. The integrated CS and SO maps do not show much correspondence. While SO is concentrated in one single clump, CS is spread over a larger area (Fig. 7). This is also visible in a direct comparison of integrated line temperatures of the individual CS and SO spectra (Fig. 8). Over a wide range of integrated SO temperatures CS shows not much variation in intensity. A direct comparison of the CS and SO profiles indicate that both molecules trace different volumes inside the cloud. The profiles look differently, the CS lines are generally broader in the $J = 2 \rightarrow 1$ and also the $3 \rightarrow 2$ line compared to the SO spectra (Fig. 6).

The relative abundances of CS and SO are thought to reflect the varying C/O ratio inside a cloud: oxygen rich clouds should have more SO, whereas carbon rich clouds should have high CS abundances (e.g. Swade 1989).

Furthermore, the abundances of both molecules are influenced by the amount of sulphur available in the gas phase; the less S is depleted onto dust grains, the higher the abundances of SO and CS are (cf. Pineau des Forêts et al. 1993). To explain SO abundances in dark clouds sulphur must be depleted by a factor of 100 (Millar & Herbst 1990). On the other hand UV spectroscopy of interstellar gas with the Copernicus satellite reveal that in diffuse clouds sulphur is essentially undepleted (Snow 1977). Our detection of strong SO in several translucent cirrus cloud (Paper I) let us suggest that with respect to the S depletion these clouds are similar to diffuse clouds. This was recently confirmed by HST observation of a star behind a translucent cloud with E_{B-V} = 0.82 mag where Snow et al. (1996) found little S depletion (less than a factor of 5).

Recently, it had been shown that abundance variations inside a cloud might be a consequence of chemical bistability (Le Boulot et al. 1995). This effect circumscribes the coexistence of two stable phases in molecular clouds, which differ mainly by the degree of ionisation, hence called the high and the low ionisation phase, HIP and LIP. Bistability affects the abundances of CS and SO: SO is predicted to be highly abundant in LIP and CS in HIP (Gerin et al. 1997). Therefore varying degree of ionisation along the line of sight can be the cause for our finding that CS and SO possibly do not fill the same volumes. Whether or not the varying SO-to-CS abundance ratio found for the clouds discussed establishes the existence of chemical bistability is beyond the scope of our observations. Clearly observations of other molecules are needed to confirm this possibility.

6. Conclusions

In this paper we have shown that sulphur monoxide is a wide spread molecule in galactic cirrus cores. For at least three clouds the emission of this molecule is extended over several arcmins. From analysis of the SO ($N_J = 1_0 \rightarrow 0_1$) line we derive SO column densities $N(\mathrm{SO}) \approx 5\ 10^{12}\mathrm{cm}^{-2}$. Based on visual extinctions estimates we derive similarly high SO abundances as

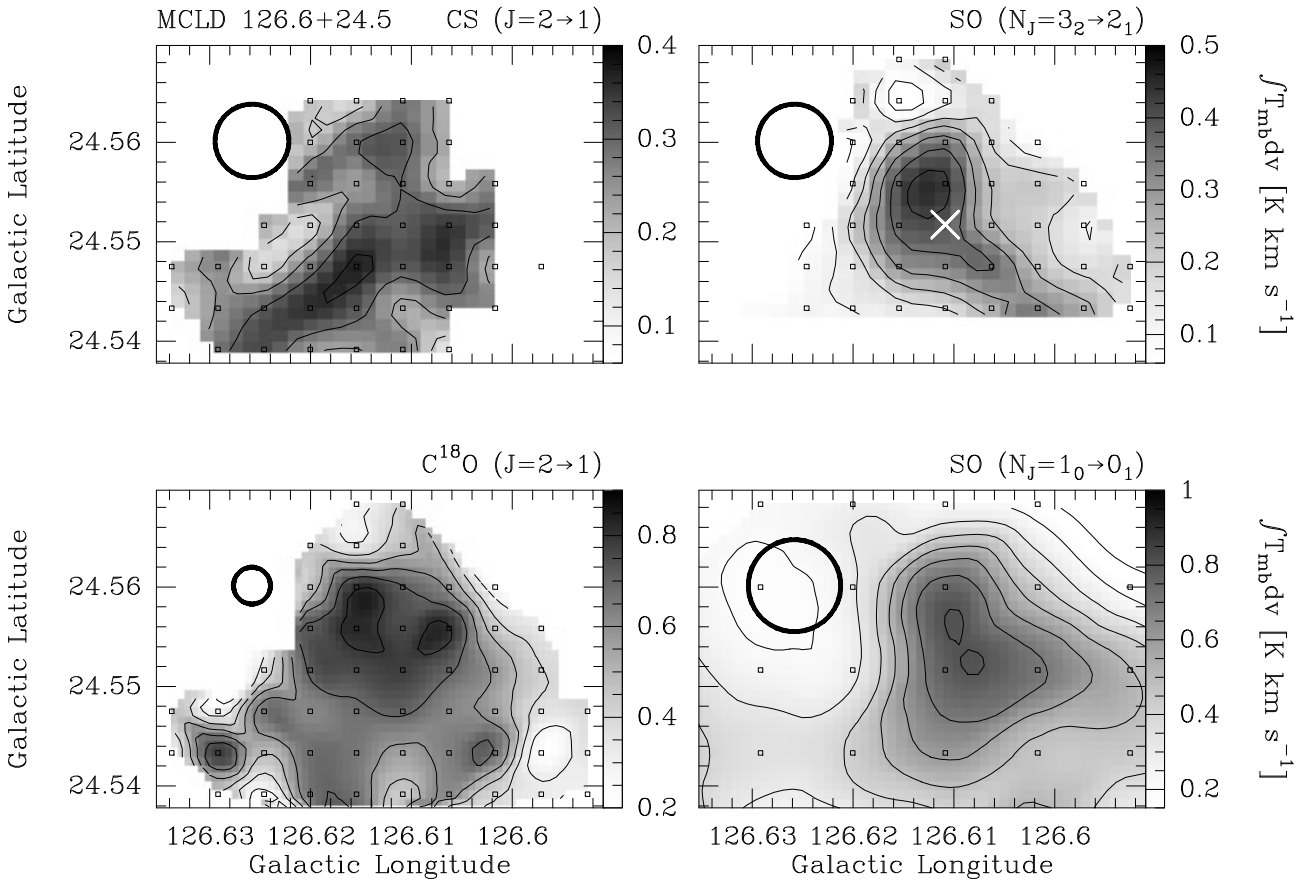

Fig. 7. Maps of integrated CS ($2 \rightarrow 1$) (top left), SO ($3_2 \rightarrow 2_1$) (top right), SO ($1_0 \rightarrow 0_1$) (bottom right), and $C^{18}O$ ($2 \rightarrow 1$) in MCLD 126.6+24.5. Contours are every 0.06 K km s^{-1} starting at 0.06 K km s^{-1} for CS and SO ($3_2 \rightarrow 2_1$), every 0.1 K km s^{-1} starting at 0.2 K km s^{-1} for $C^{18}O$ and SO ($1_0 \rightarrow 0_1$). The beam size is indicated in the top left corner of the maps. Observed positions are indicated by open squares. The X in the SO ($3_2 \rightarrow 2_1$) map marks the position with the maximum SO temperature at $\Delta l = -210''$, $\Delta b = 60''$ discussed in the text.

Table 5. Column densities

Source	N(CS) (10^{12}cm^{-2})	N(SO) (10^{12}cm^{-2})	$\frac{N(\mathrm{CS})}{N(\mathrm{SO})}$
Draco[a]	< 0.4	3.3	< 0.12
LVC 127+20[a]	< 0.4	7.8	< 0.05
MCLD 126.6+24.5[a]	2	10	0.2
MCLD 126.6+24.5[b]	$15 - 45$	$10 - 30$	$0.5 - 4.5$
MBM 32[a]	0.7	4.6	0.15
MCLD 123.5+24.9[c]	$6 - 25$	8	$0.8 - 3$
L134N[d]			0.05[e]
TMC1[d]			2

Remarks: *a*: LTE results, *b*: based on escape probabilty model with uncertain N(CS). *c*: taken from Gerin et al. (1997; *d*: from Irvine et al. (1987, *e*: varying with position (Swade 1989)

for the previously detected cirrus clouds (Paper I). Similarly as the analysis of Turner (1995) we find that all sulphur must be essentially in the gas phase to explain the amount of SO detected.

In contrast to the SO study of Turner (1995) our extensive mapping of the SO ($N_J = 1_0 \rightarrow 0_1$) line towards MCLD 126.6+24.5, one of Turner's targets sources, shows that this core is neither simply stuctured, nor symmetric. It rather can be subdivided into smaller substructures or clumps. These clumps follow similar size-line width and size-density relations as found for cirrus clouds as whole entities (Heithausen 1996).

For the largest clump in MCLD 126.6+24.5 we present a detailed study of the excitation and distribution of CS and SO. Based on the analysis of the line profiles and the integrated maps of both molecules we find that CS seems to be wider spread than SO in MCLD 126.6+24.5; SO is concentrated in small clumps. Our excitation study of SO confirms previous estimates on the SO column density; the SO abundance must be high in cirrus clouds.

The comparison of CS and SO towards MBM 32, LVC-127+20, and the Draco cloud shows that SO is more abundant than CS by possible a factor of 10. For MCLD 126.6+24.5 we find an [CS]/[SO] $\leq$ 1. Due to the differences in the profiles of CS and SO in MCLD 126.6+24.5 we conclude that both molecules do not necessarily trace the same volume inside the cloud. There is no correlation between the column densities of both molecules, thus the abundance ratio of the molecules is varying with position. These findings together with the clumpy

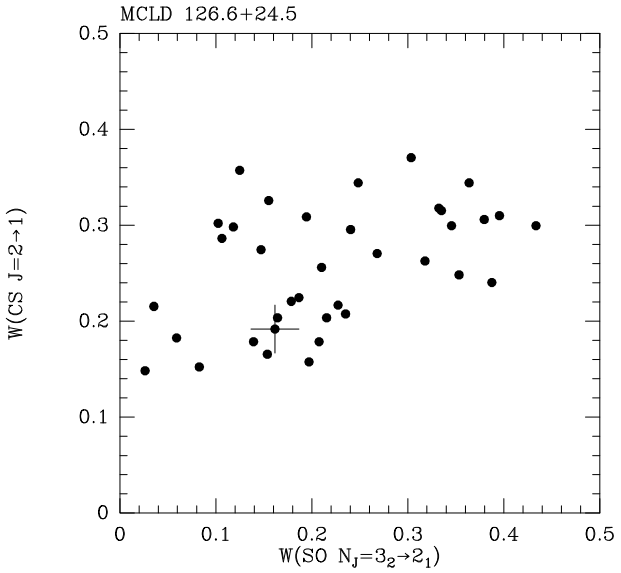

Fig. 8. Comparison of the integrated line temperatures of the CS (2→ 1) and the SO ($3_2 \rightarrow 2_1$) transitions in MCLD 126.6+24.5. The cross indicates an 1σ error bar.

structure of the clouds make it questionable whether simple polytropic hydostatic equilibrium models (Turner 1995, 1996) are sufficient or rather clumpy cloud models as e.g. developed by Spaans (1996) are needed to properly describe the physical and chemical state of cirrus clouds.

Acknowledgements. We thank Peter Schilke for critically reading the manuscript. This study was partly supported by the Deutsche Forschungsgemeinschaft (DFG) grant SFB 301.

References

Boden K.-P., Heithausen A. 1993, A&A 268, 255
Corneliussen U., 1996, PhD thesis, University of Cologne
Drdla K., Knapp G.R., van Dishoeck E.F., 1989, ApJ 345, 815
Elmegreen B.G., Falgarone E., 1996, ApJ 471, 816
Gerin M, Falgarone E., Joulain K., Kopp M., Le Bourlot J., Pineau des Forêts G., Roueff E., Schilke P., 1997, A&A 318, 579
Goldsmith P.F., 1991, in *IAU SYmp. 147: Fragmentation of Molecular Clouds and Star Formation*, Eds. E. Falgarone, F. Boulanger & G. Duvert, p. 177
Großmann V., Heithausen A., Corneliussen U., 1997 (in prep.)
Heithausen A., Mebold U., de Vries H.W., 1987, A&A 179, 263
Heithausen A., Mebold U., 1989, A&A 214, 347
Heithausen A., Stacy J.G., de Vries H.W., Mebold U., Thaddeus P., 1993, A&A 268, 265
Heithausen A., Corneliussen U., Großmann V., 1995, A&A 301, 941, (Paper I)
Heithausen A., 1996, A&A 314, 251
Irvine, W.M., Goldsmith, P.F., Hjalmarson, A, 1987, In: *Interstellar Processes*, Eds. D.J. Hollenbach & H.A. Thronson, p. 561
Kramer C., Wild W., 1994, IRAM Newsletter 18, 2
Le Bourlot J., Pineau des Forêts G., Roueff E., 1995, A&A 297, 251
Mebold U., Cernicharo J., Velden L., Reif K., Crezelius C., Goerigk W. 1985, A&A 151, 427
Mebold U., Heithausen A., Reif K., 1987, A&A 180, 213
Meyerdierks H., Brouillet N., Mebold U., 1990, A&A 230, 172
Millar T.J., Herbst E., 1990, A&A 231, 466
Ott M., Witzel A., Quirrenbach A., Krichbaum T.P., Standke C.J., Schalinski C.J., Hummel C.A., 1994, A&A 284, 331
Pineau des Forêts G., Roueff E., Schilke P., Flower D.R., 1993, MNRAS 262, 915
Prasad S.S., Huntress W.T., 1982, ApJ 260, 590
Reach W.T., Pound M.W., Wilner D.J., Lee Y., 1995, ApJ 441,244
Scalo J., 1985, in *Protostars and Planets*, Eds. D.C. Black & M. S. Matthews, Univ. of Arizona Press, Tucson, p. 201
Schreiber W., Wouterloot J.G.A., Heithausen A., Winnewisser G., 1993, A&A 276, L5
Snow T.P., 1977, ApJ 216, 724
Snow T.P., Black J.H., van Dishoeck E.F., Burks G., Crutcher R.M. Lutz B.L., Hanson M.M., Shuping R.Y., 1996, ApJ 465, 245
Spaans, M., 1996, A&A 307, 271
Stutzki J., Güsten R., 1990, ApJ 356, 513
Swade D.A., 1989, ApJ 345, 828
Turner B.E., 1995, ApJ 455, 556
Turner B.E., 1996, ApJ 461, 246
Ungerechts H., Bergin E.A., Goldsmith P.F., Irvine W.M., Schloerb F.P., Snell R.L., 1995, in "*The physics and chemistry of interstellar molecular clouds*", Eds. G. Winnewisser & G. Pelz, Springer Verlag, New York, p. 258

This article was processed by the author using Springer-Verlag LaTeX A&A style file *L-AA* version 3.